Check for updates

*CORRESPONDENCE
Yihong Yang
✉ yihongyang@intra.nida.nih.gov
Chaozhe Zhu
✉ czzhu@bnu.edu.cn

†These authors have contributed
equally to this work

Targeting the pathological network: Feasibility of network-based optimization of transcranial magnetic stimulation coil placement for treatment of psychiatric disorders

Zhengcao Cao[1†], Xiang Xiao[1,2†], Yang Zhao[1], Yihan Jiang[1], Cong Xie[1], Marie-Laure Paillère-Martinot[3,4], Eric Artiges[4,5], Zheng Li[6,7], Zafiris J. Daskalakis[8], Yihong Yang[2]* and Chaozhe Zhu[1,7,9]*

[1]State Key Laboratory of Cognitive Neuroscience and Learning, Beijing Normal University, Beijing, China, [2]Neuroimaging Research Branch, National Institute on Drug Abuse, National Institutes of Health, Baltimore, MD, United States, [3]Department of Child and Adolescent Psychiatry, Pitié-Salpêtrière Hospital, APHP.Sorbonne Université, Paris, France, [4]INSERM U A10 Developmental Trajectories and Psychiatry, Ecole Normale Supérieure Paris-Saclay, CNRS, Center Borelli, University of Paris-Saclay, Gif-sur-Yvette, France, [5]Department of Psychiatry, Etablissement Public de Santé (EPS) Barthélemy Durand, Étampes, France, [6]State Key Laboratory of Cognitive Neuroscience and Learning, Center for Cognition and Neuroergonomics, Beijing Normal University at Zhuhai, Zhuhai, China, [7]IDG/McGovern Institute for Brain Research, Beijing Normal University, Beijing, China, [8]Department of Psychiatry, University of California, San Diego, La Jolla, CA, United States, [9]Center for Collaboration and Innovation in Brain and Learning Sciences, Beijing Normal University, Beijing, China

It has been recognized that the efficacy of TMS-based modulation may depend on the network profile of the stimulated regions throughout the brain. However, what profile of this stimulation network optimally benefits treatment outcomes is yet to be addressed. The answer to the question is crucial for informing network-based optimization of stimulation parameters, such as coil placement, in TMS treatments. In this study, we aimed to investigate the feasibility of taking a disease-specific network as the target of stimulation network for guiding individualized coil placement in TMS treatments. We present here a novel network-based model for TMS targeting of the pathological network. First, combining E-field modeling and resting-state functional connectivity, stimulation networks were modeled from locations and orientations of the TMS coil. Second, the spatial anti-correlation between the stimulation network and the pathological network of a given disease was hypothesized to predict the treatment outcome. The proposed model was validated to predict treatment efficacy from the position and orientation of TMS coils in two depression cohorts and one schizophrenia cohort with auditory verbal hallucinations. We further demonstrate the utility

of the proposed model in guiding individualized TMS treatment for psychiatric disorders. In this proof-of-concept study, we demonstrated the feasibility of the novel network-based targeting strategy that uses the whole-brain, system-level abnormality of a specific psychiatric disease as a target. Results based on empirical data suggest that the strategy may potentially be utilized to identify individualized coil parameters for maximal therapeutic effects.

Highlights

- Proposed a model of targeting pathological brain networks for pre-treatment TMS coil placement planning in the treatment of psychiatric disorders.
- Validated the network targeting model in three cohorts of patients with depression or auditory verbal hallucinations, *via* prediction of individual TMS treatment efficacy from the parameters of coil placement.
- Demonstrated the utility of the network targeting model in guiding individualized TMS coil placement.

1 Introduction

Transcranial magnetic stimulation (TMS) is a noninvasive neuromodulation technology that can modulate neural activity with spatial sensitivity of ∼1 cm (Barker et al., 1985; De Deng et al., 2013). Accumulating evidence has shown its potential as a clinical therapy for many psychiatric disorders (Rossini et al., 2010; Lefaucheur et al., 2014; Sale et al., 2015). However, the large variation in treatment efficacy across diseases and individual patients underscores the importance to improve the current TMS treatment protocols.

In TMS-based treatment, a major methodological issue is how to achieve optimal efficacy by choosing the parameters, particularly the position and orientation of the TMS coil (Fitzgerald, 2021). Traditionally, TMS coils are placed according to anatomically defined regions, e.g., dorsolateral prefrontal cortex (DLPFC) for major depressive disorder (MDD). TMS coils are usually placed on a specific site, e.g., 5-cm from the motor hotspot (George et al., 1994; Pascual-Leone et al., 1996), referring to scalp landmarks of the EEG 10–20 system (Herwig et al., 2003; Beam et al., 2009), or projecting to brain coordinates *via* a neuronavigation system (Herwig et al., 2001; Fitzgerald et al., 2009). However, the location of region-of-interest (ROI) alone is insufficient for guiding the optimal setting of TMS coils. First, within the targeted ROI, the distribution of the E-field

generated by TMS further depends on the pose of the TMS coil relative to the gyrification of cortex underneath (Richter et al., 2013; Gomez-Tames et al., 2018). Accordingly, it is necessary to consider the location-and-orientation interaction when placing TMS coils for optimal outcomes, even in the case of motor-evoked potentials (Reijonen et al., 2020). Second, the treatment response of TMS may further depend on the specific functional network associated with cortical regions directly affected by the stimulation. TMS is capable of generating effects in remote brain regions connected to the local stimulating site (Bestmann et al., 2008; Eldaief et al., 2011; Reithler et al., 2011; Tik et al., 2017). Effective treatments are found to be accompanied by stimulation-induced changes in brain activity that occur in the downstream regions or their functional connectivity with the local region (Wang et al., 2014; Cash et al., 2019; Howard et al., 2020). Therefore, even when a given ROI is targeted, distinct functional networks can be affected by TMS in different individuals, and such variation of stimulation networks may account for the heterogeneity of the treatment response (Opitz et al., 2016; Cardenas et al., 2022). Resolving how the stimulation network mediates the relationship between the coil settings and the treatment outcome is critical for guiding the individualized optimization of TMS parameters.

For modeling the whole brain profile of the stimulation network from coil settings on an individual's scalp, a previous work by Opitz et al. (2016) described a general framework integrating the realistic E-field modeling (Windhoff et al., 2013) and resting-state functional connectivity (rsFC) mapping (Fox and Raichle, 2007; Fox et al., 2012, 2014). This framework allows one to address TMS targeting at the network level. In a healthy cohort, this framework demonstrated how the stimulation networks vary among individuals when DLPFC was selected for treating MDD. However, it remains unclear what stimulation network profile will optimally benefit the clinical/behavioral outcome, which is crucial in guiding treatment for psychiatric disorders.

For determining beneficial stimulation network profiles, a "pathological network" of a specific psychiatric disease (e.g., the difference in brain activity between patients and controls)

may serve as a potential target. Psychiatric disorders have been recognized as network disruptions (Silbersweig et al., 1995; Mayberg, 1997; Fornito and Bullmore, 2015; Braun et al., 2018). In MDD, multiple cortical and limbic nodes showing abnormal activity compared to healthy controls have been recognized to underpin the disease. Seminal research in depression has found that stimulation sites with stronger negative functional connectivity to the subgenual cingulate cortex (SGC), one deep node of the putative frontal-limbic network of depression, bear better treatment outcomes (Fox et al., 2012; Weigand et al., 2018). These findings inspire a hypothesis that the association between the stimulation network and the pathological network of a given disease may mediate the outcome drawn by TMS.

Based on this hypothesis, we propose a novel network targeting model for guiding individualized coil settings in treating psychiatric disorders. We first validated the feasibility of the proposed model in predicting treatment efficacy from TMS coil settings on individual scalps retrospectively on two cohorts of depression. Then, we further validated the feasibility to generalize this model to another disease, schizophrenia with auditory verbal hallucinations (AVH). Finally, we demonstrated that optimized coil placement parameters vary between individual patients, which emphasizes the importance of individualized coil placement in TMS-based treatment.

2 Materials and methods

2.1 Description of the network targeting model

2.1.1 Rationale of the model

The proposed model is based on the relationship between two conceptional networks: the stimulation network and the pathological network of a given disease. In the current scope, TMS parameters are limited to the position and orientation of TMS coil, and treatment outcome is defined by the change of disease severity measured with clinical scales. For a given setting of TMS coil parameters (**Figure 1A**i), the TMS stimulation region is defined as the cortical region that is directly modulated by TMS, and estimated from finite element model (FEM) based on the individual's structural MRIs (**Figure 1A**ii). Then the stimulation network, defined as the profile of the whole-brain rsFC seeded from the stimulation region, was estimated from the voxel-wise connectome averaged from a large sample healthy cohort (**Figures 1A**iii, iv). Individuals showing spatial anti-correlations between their stimulation networks (**Figure 1B**) and the pathological network of a given disease (**Figure 1C**) are hypothesized to be associated with effective treatment by TMS (Fox et al., 2014; **Figure 1D**).

2.1.2 Parameter space

We utilized a scalp geometry-based parameter space that describes any possible TMS coil placement with two key parameters (position s and orientation θ) on the individual scalp surface (Jiang et al., 2022). The description of position s is a pair of coordinates (p_{NZ}, p_{AL}) on a continuous proportional coordinate system (CPC), where p_{NZ} indicates the position along nasion to inion direction, p_{AL} indicates the position along with left preauricular point (AL) to right preauricular point (AR) direction, and (p_{NZ} and p_{AL}) $\in$[0 1] $\times$ [0 1] (Xiao et al., 2018). The coil orientation (of the handle) is defined in the tangent plane of position s. There are two steps to define the direction of orientation 0°. First, we find the intersecting line between the tangent plane and the plane through position s, AL, and AR. Second, the 0° direction originates from position s, perpendicular to the intersecting line, and points backward. The description of orientation θ is the rotation angle from orientation 0° to the coil handle. For clockwise rotation, θ $\in$($-180°$ to 0°). For anti-clockwise rotation, $\theta \in$(0° to 180°). In practice, both parameters of s and θ can be implemented with manual measurement (Jiang et al., 2022) and computer-assistant navigation (Xiao et al., 2018; Jiang et al., 2022).

2.1.3 Local effects of TMS stimulation

For a given location and orientation, the local region affected by the TMS induced E-field was estimated by applying FEM modeling on the individual's T1 image. The FEM modeling was implemented using SimNIBS (Thielscher et al., 2011). According to putative assumptions on the TMS excitatory/inhibitory mechanism, TMS induces an excitatory effect when the pulses are repeatedly delivered at a high frequency (HF) of > 5 HZ, while an inhibitory effect is induced at a low frequency (LF) of $\leq$ 1 HZ (Pascual-Leone et al., 1998; Dayan et al., 2013).

Such an excitatory/inhibitory effect is limited to the E-field region under coil *para (s, θ)*. Assuming a brain with N voxels in standard brain space, the local effect of TMS stimulation can be described by an N-by-1 vector E_l.

$$E_l\,(s,\,\theta)\;=\;[V_i]'\;=\;\begin{cases} w, Excitory\ stimulation \\ -w, Inhibitory\ stimulation \\ \quad 0,\quad Otherwise \end{cases}$$

$$(1)$$

Here, V_i is the local effect of TMS induced on the ith voxel in the E-field region, and w is the weight of E-field strength.

2.1.4 RS-FC profile of TMS stimulation (stimulation network)

In the current model, the rsFC profile of the stimulated region was estimated from the group-level rsFC matrix of the healthy cohort (Weigand et al., 2018). Specifically, the regional

FIGURE 1
Schematic illustration of network targeting model. **(A)** Stimulation network. For transcranial magnetic stimulation (TMS) administrated with a given combination of parameters (i), the generated E-filed (ii) defines direct TMS effects on the local cortical region. Group-level rsFC (iii) provides a visualization of the functional network affected *via* the stimulated cortical region, i.e., the stimulation network (iv). **(B)** Stimulation networks vary among individuals due to both the coil setting and geometry and productivity of individuals' intra-cranial tissues. **(C)** Comparing to the pathological network of a given disease, **(D)** stimulation networks showing spatial anti-correlation are hypothesized to be associated with better clinical improvement induced by TMS (Fox et al., 2014).

rsFC profile, i.e., the "stimulation network," was calculated from the weighted average of whole-brain rsFC seeded from each voxel within the E-field region. The stimulation network corresponding to *para (s, θ)* is given by:

$$E_n(s, \theta) \ = \ C \cdot E_l(s, \theta)/||E_l(s, \theta)||_1 \qquad (2)$$

Here, C describes the voxel-wise rsFC matrix, and $E_l(s, \theta)$ is the local effect of *para (s, θ)*, and $|| \quad ||_1$ is the 1-norm of a vector, such that E-field weight of suprathreshold voxels sum to one. For N gray-matter voxels in MNI space, C is given by:

$$C \ = \ \begin{bmatrix} c_{ij} \end{bmatrix}, \quad i, j \ = \ 1, 2, ..., N \qquad (3)$$

where c_{ij} is the signed rsFC strength between voxels i and j.

In the current study, the group-level rsFC was estimated from high-resolution T1 MR images and 8-min resting-state fMRI data of 512 healthy young adults [225 females, age 20.12 ± 1.28 years] from the SLIM database (Liu et al., 2017). The processing of MRI data is detailed in the **Supplementary material**.

2.1.5 Network targeting accuracy

In the proposed model, the metabolic hypo-/hyper-activity was taken as the biological marker for the pathological network of a particular psychiatric disorder. To describe the pathological

network, we utilized an image generated from the coordinates-based meta-analysis (CBMA) contrasting a cohort of patients vs. healthy controls (Kühn and Gallinat, 2012; Fox et al., 2014; Gray et al., 2020). Assuming that the whole gray matter of the brain consists of N voxels in its functional image, which constitute a brain network, the combined activity of these brain voxels represents a state of the brain. The brain states of the patients and controls are represented in N × 1 vectors I_{pt} and I_{hc}, respectively, and the difference between the two states is:

$$P \ = \ I_{pt} - I_{hc} \qquad (4)$$

According to the finding that excitatory/inhibitory stimulation on negative/positive FC from the local ROI to deep pathological nodes is beneficial to TMS efficacy (Fox et al., 2014), we extended this principle by defining the spatial anti-correlation between the pathological network and the TMS stimulation network as the network targeting accuracy (NTA), which we hypothesize can predict the treatment outcome of TMS. For the given para (s, θ), the NTA can be quantified by:

$$NTA \ (s, \theta) \ = \ -corr < E_n(s, \theta), P > \qquad (5)$$

In the current study, we separately utilized the results of two recent CBMA studies as the descriptions of pathological

networks for MDD (Gray et al., 2020) and schizophrenia with AVH (Kühn and Gallinat, 2012).

2.2 Proof-of-concept validation

We conducted three validation experiments to evaluate the feasibility of the proposed NTA model in predicting TMS efficacy from the coil parameters.

First, we tested whether NTA explains the equation-based efficacy (Herbsman et al., 2009; Fox et al., 2012) of empirical DLPFC sites used in treatment of MDD (Rajkowska and Goldman-Rakic, 1995; Paus et al., 2001; Herwig et al., 2003; Okamoto et al., 2004; Cho and Strafella, 2009; Fitzgerald et al., 2009; Herbsman et al., 2009; Rusjan et al., 2010; Fox et al., 2012; Weigand et al., 2018; Cash et al., 2019). Coil settings described in above literatuals were simulated on T1 images of 68 depression patients [49 females, age 23.69 ± 8.17 years] obtained from OpenNeuro (Anna Manelis et al., 2021; Liuzzi et al., 2021). We calculated site-wise NTA and compared them to the estimated efficacy by Herbsman's equation (Herbsman et al., 2009).

Second, to confirm that the NTA model is capable of predicting the efficacy in the clinical treatment of MDD, we conducted a retrospective validation on a cohort of 33 MDD patients [20 females, age 47.70 ± 7.54 years] who received a 2-week treatment of 10 Hz high-frequency rTMS in a previous study (Paillère Martinot et al., 2010). Treatment was targeted using the 5-cm rule or PET-based navigation. We split the 33 patients into two groups (Fox et al., 2012), the left PFC group (N = 27) and the right PFC group (N = 6). Using the coil settings recorded from the TMS treatments, we implemented the proposed model on the patients' T1 image and calculated NTA. The calculated NTA was correlated with the actual clinical improvement in each group.

Finally, to test whether the NTA model can be generalized to diseases other than MDD, we conducted another retrospective validation on a cohort of 15 schizophrenia [7 females, age 32.07 ± 6.79 years] who received 10 days of 1-Hz rTMS treatment for their AVH symptom (Paillère-Martinot et al., 2017). Treatment was targeted using fMRI-based navigation. Again, we implemented the NTA model on each patient's T1 image and calculated NTA from the recorded coil parameters. The calculated NTA was correlated with the actual clinical improvement of each patient.

For each subject in the three corhorts, we first segmented T1 images of these patients using SimNIBS 3.2 (Thielscher et al., 2015; Saturnino et al., 2019). On the scalp surface, position and orientation of TMS coil was simulated on the extracted scalp according to the description of treatment protocol or parameters recorded with neuronavigation system. From the simulated TMS coil, the E-field distribution on individual cortex was estimated using the FEM of SimNIBS 3.2. The E-field weighted group-level function connectivity

seeded in the affected cortical area was used to estimate the stimulation network of TMS according to equation 2. For each disorder of MDD and schizophrenia with AVH, we derived the image of pathological network from the result of large-sampled meta-analyses, (Gray et al., 2020) for MDD (**Supplementary Table 1**) and (Kühn and Gallinat, 2012) for schizophrenia with AVH (**Supplementary Table 2**). Finally according to the equation 5, NTA for the targeted pathological network was calculated for each of the patients, and correlated with the treatment outcome of TMS either estimated from the empirical equation or recorded from clinical treatment trials.

The full methodology is detailed in the **Supplementary material**.

2.3 Individualized parameter optimization

Motivated by the results of the above analyses, which showed that NTA is able to predict TMS treatment efficacy from the coil parameters, we propose that NTA may serve as an objective function for the individualized optimization of coil parameters. We conducted simulation experiments to demonstrate how optimal parameters vary across patients.

Simulation experiments were conducted on the cohorts of MDD and schizophrenia with AVH (Paillère Martinot et al., 2010; Paillère-Martinot et al., 2017). In each cohort, we defined a cranial search space covering traditional TMS sites for the two diseases. For MDD the search space had 125 positions × 12 orientations and covered a broad area of left DLPFC (Lefaucheur et al., 2014; Xiao et al., 2018; Cash et al., 2020; Balderston et al., 2021). For schizophrenia with AVH, the search space had 122 positions × 12 orientations and covered a broad area including left superior temporal gyrus (STG) and left temporoparietal junction (TPJ), which have been adopted in TMS treatments for schizophrenia with AVH (Hoffman et al., 2003, 2013; Klirova et al., 2013; Lefaucheur et al., 2014; Paillère-Martinot et al., 2017; Xiao et al., 2018). We calculated disease-specific NTA values for each of the parameter combinations, and define the individualized optimal TMS parameters as the combination with maximum NTA.

The full methodology is detailed in the **Supplementary material**.

3 Results

3.1 Correlation between NTA and equation-based clinical efficacy

To test the hypothesis that NTA predicts treatment efficacy for MDD, we compared NTA and the expected treatment

efficacy among 12 TMS sites used for treating MDD (**Figure 2A**, **Supplementary Tables 3, 4**), sourced from previous reviews (Fox et al., 2012; Cash et al., 2020). For each of the cortical targets, the corresponding scalp position was first identified by finding the scalp position with a normal vector pointing to the cortical target, then orientation was fixed at 45° from the mid-line (Fitzgerald et al., 2003; Thomson et al., 2013; **Figure 2B**; and **Supplementary Figure 1**). The parameters of the coil were therefore simulated on each of the 68 individuals from the first cohort. For each cortical site, the across-individual distribution of NTA is shown in **Figure 2C**, and the mean NTA was used to predict the treatment efficacy estimated with Herbsman's equation (Herbsman et al., 2009). Across stimulating sites, the NTA showed a significant correlation with Hamilton Depression Rating Scale (HDRS) total improvement ($N = 68$, $r = 0.923$, $p = 9.32 \times 10^{-6}$, one-tailed) and explained about 85% of the variance assessed by HDRS (**Figure 2D**). Furthermore, such predictiveness was significantly higher than network targeting models based on randomly generated networks (10^5 permutation runs, $p = 0.0343$, **Supplementary Figure 2**) and was significantly higher than prediction based on randomly reassigned clinical outcomes (10^5 permutation runs, $p = 3 \times 10^{-5}$, **Supplementary Figure 3**). Additionally, the estimated NTA is stable when the E-field threshold varied in a range of 75–99% ($r > 0.9$, **Supplementary Figure 4**) and when the radius of the pathological network foci varied in a range of 4–16 mm ($r > 0.9$, **Supplementary Figure 5**).

3.2 Correlation between NTA and treatment efficacy on MDD patients

In the MDD cohort who received TMS treatment, the recorded TMS coil positions and orientations are shown in **Figure 3A** and listed in (**Supplementary Table 5**). Across stimulating sites in left PFC (Fox et al., 2012), NTA showed a significant correlation with Montgomery–Asberg Depression Rating Scale (MADRS) total improvement ($N = 27$, $r = 0.337$, $p = 0.043$, one-tailed) and explained about 11% of the variance assessed by MADRS (**Figure 3B**). Furthermore, such predictiveness was significantly higher than network targeting models based on randomly generated networks (10^5 permutation runs, $p = 0.0306$, **Supplementary Figure 2**) and was significantly higher than prediction based on randomly reassigned clinical outcomes (10^5 permutation runs, $p = 0.0355$, **Supplementary Figure 3**). Additionally, NTA was stable when the E-field threshold varied in a range of 75–99% ($r > 0.9$, **Supplementary Figure 4**) and when the radius of the pathological network foci varied in a range of 4–16 mm ($r > 0.9$, **Supplementary Figure 5**). In this cohort, sex and age did not show significant correlation with the clinical outcome (Sex: $r = -0.295$, $p = 0.068$, one-tailed; Age: $r = 0.261$, $p = 0.094$, one-tailed). The correlation between NTA and MDD treatment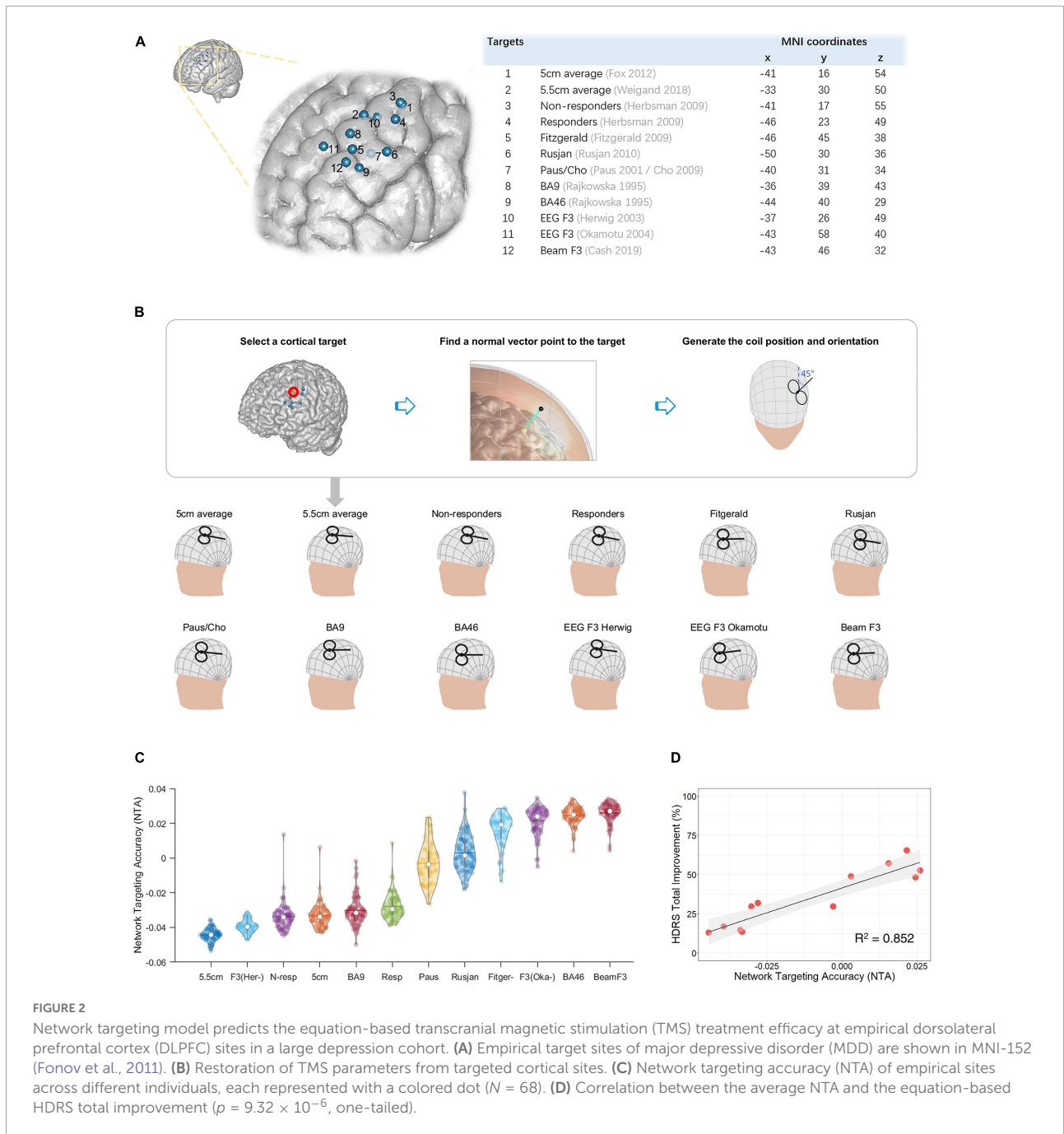 outcome was impacted by demographic factors such as sex (partial correlation $r = 0.228$, $p = 0.131$, one-tailed) and age ($r = 0.288$, $p = 0.077$, one-tailed).

The predictiveness of the NTA model was limited within the left PFC. For the six other patients in this cohort who received high-frequency TMS treatment in the right PFC, their clinical outcome was not predicted by the NTA model ($N = 6$, $r = -0.310$, $p = 0.725$, one-tailed, **Supplementary Figures 6, 7**). This result may due to that the treatment outcome in these subjects come from a placebo effect rather than the TMS modulation, given evidence that the anti-MDD efficacy of high-frequency rTMS is specific to left DLPFC (Lefaucheur et al., 2014).

3.3 Correlation between NTA and treatment efficacy on schizophrenia patients with AVH

TMS coil positions and orientations of the active group are shown in **Figure 4A** and listed in (**Supplementary Table 6**). Across stimulating sites, NTA showed a significant correlation with Auditory Hallucination Rating Scale (AHRS) total improvement ($N = 15$, $r = 0.556$, $p = 0.016$, one-tailed) and explained about 31% of the variance assessed by AHRS (**Figure 4B**). Furthermore, such predictiveness was significantly higher than network targeting models based on randomly generated networks (10^5 permutation runs, $p = 0.0042$, **Supplementary Figure 2**) and was significantly higher than prediction based on randomly reassigned clinical outcomes (10^5 permutation runs, $p = 0.0176$, **Supplementary Figure 3**). Additionally, the estimated NTA was stable when the E-field threshold varied in a range of 75–99% ($r > 0.8$, **Supplementary Figure 4**) and when the radius of pathological network foci varied in a range of 4–16 mm ($r > 0.9$, **Supplementary Figure 5**). In this cohort, sex and age did not show significant correlation with the clinical outcome (Sex: $r = -0.036$, $p = 0.449$, one-tailed; Age: $r = 0.369$, $p = 0.088$, one-tailed). The correlation between NTA and schizophrenia treatment outcome was not impacted by demographic factors such as sex (partial correlation $r = 0.557$, $p = 0.019$, one-tailed) and age ($r = 0.489$, $p = 0.038$, one-tailed).

We further correlated NTA with changes in other clinical assessments, including scales of schizophrenia, the Scale for the Assessment of Positive Symptoms (SAPS) and the Scale for the Assessment of Negative Symptoms (SANS)(**Table 1**). First, the predictiveness of NTA showed specificity to TMS induced changes in positive symptoms ($N = 15$, $r = 0.572$, $p = 0.013$, one-tailed) but not in negative symptoms ($N = 15$, $r = 0.021$, $p = 0.470$, one-tailed). Second, within the sub-scales of SAPS, NTA predicted changes in hallucination-related items, but not in other items related to delusion, bizarre behavior, and positive formal thought disorder. Collectively, the above
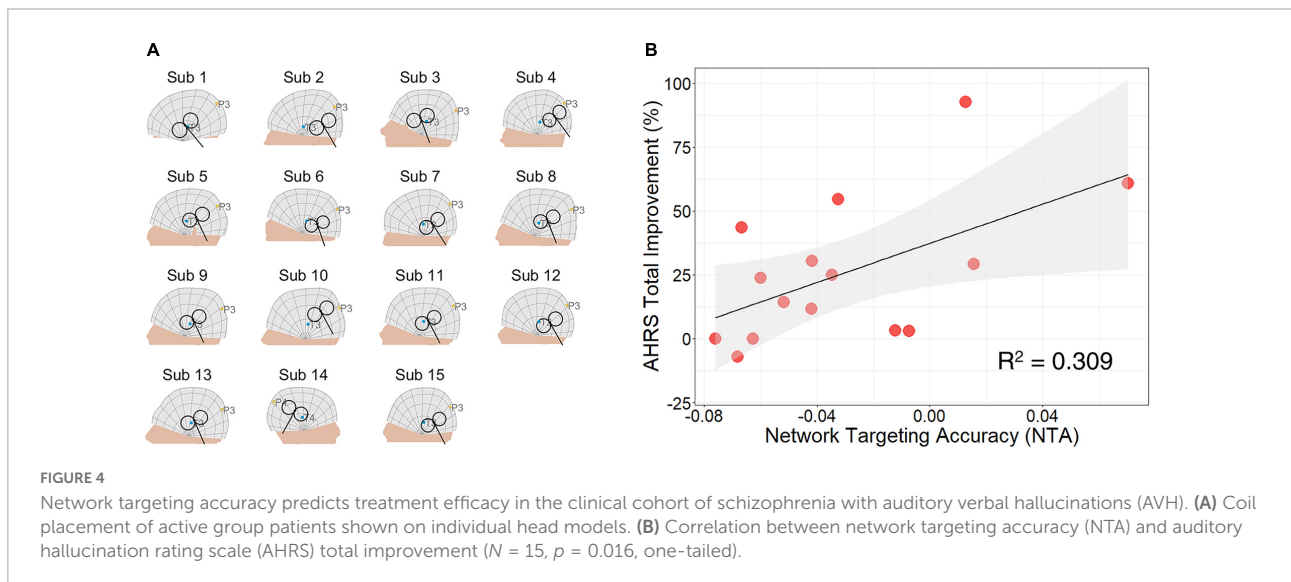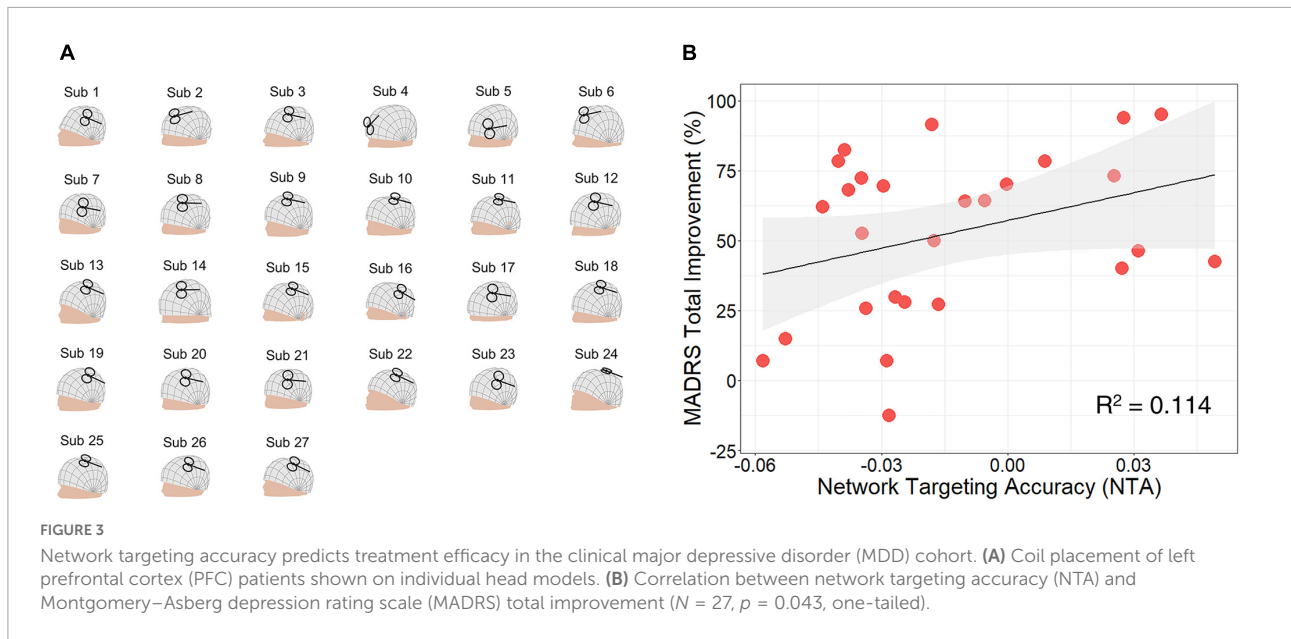
FIGURE 2

Network targeting model predicts the equation-based transcranial magnetic stimulation (TMS) treatment efficacy at empirical dorsolateral prefrontal cortex (DLPFC) sites in a large depression cohort. **(A)** Empirical target sites of major depressive disorder (MDD) are shown in MNI-152 (Fonov et al., 2011). **(B)** Restoration of TMS parameters from targeted cortical sites. **(C)** Network targeting accuracy (NTA) of empirical sites across different individuals, each represented with a colored dot ($N = 68$). **(D)** Correlation between the average NTA and the equation-based HDRS total improvement ($p = 9.32 \times 10^{-6}$, one-tailed).

results indicate predictiveness of NTA is specific to the targeted symptom.

3.4 Position-orientation interaction on estimated treatment efficacy and individualized optimization

In the MDD cohort, we simulated the NTA model for MDD on each patient within the left DLPFC (Figure 5A,

Supplementary Table 7). Possible combinations of position and orientation formed a 2-D parameter space which was subdivided into a 125-by-12 (position by orientation) grid. We calculated the estimated NTA for each of the combinations. Across the 27 individuals, both the position [$F(124, 38974) = 375.490$, $p < 0.001$] and orientation [$F(11, 38974) = 4.201$, $p < 0.001$] had significant main effect on NTA; there was also a significant interaction effect [$F(1364, 38974) = 16.766$, $p < 0.001$] between the two parameters. Within the left DLPFC, the optimal parameter was defined as the combination with the highest value

FIGURE 3
Network targeting accuracy predicts treatment efficacy in the clinical major depressive disorder (MDD) cohort. **(A)** Coil placement of left prefrontal cortex (PFC) patients shown on individual head models. **(B)** Correlation between network targeting accuracy (NTA) and Montgomery−Asberg depression rating scale (MADRS) total improvement ($N = 27$, $p = 0.043$, one−tailed).

FIGURE 4
Network targeting accuracy predicts treatment efficacy in the clinical cohort of schizophrenia with auditory verbal hallucinations (AVH). **(A)** Coil placement of active group patients shown on individual head models. **(B)** Correlation between network targeting accuracy (NTA) and auditory hallucination rating scale (AHRS) total improvement ($N = 15$, $p = 0.016$, one−tailed).

of NTA (**Figure 5B**). Optimal parameters varied across different individuals (**Figures 5C**, **D**, **Supplementary Table 8**).

In the cohort of schizophrenia with AVH, we performed a similar simulation on a 122-by-12 (position by orientation) parameter space covering left STG and left TPJ, places where TMS is commonly administrated (**Figure 6A**, **Supplementary Table 9**). Again, we found significant main effects in both parameters of position [$F(121, 20482) = 102.572$, $p < 0.001$] and orientation [$F(11, 20482) = 11.146$, $p < 0.001$], and interaction between the two parameters [$F(1331, 20482) = 9.220$, $p < 0.001$]. **Figure 6B** illustrates the distribution of NTA and optimal parameters in a representative individual. Optimal parameters also varied among different individuals (**Figures 6C**, **D**, **Supplementary Table 10**).

4 Discussion

In this work, we proposed a novel network targeting model for guiding individualized TMS coil settings for the treatment of psychiatric disorders. The model linked the TMS parameter space of coil position and orientation with the improvement of clinical symptoms after treatment, with a hypothesis that the treatment outcome was associated with the extent of modulation by TMS on the whole pathological network of a given disease. For a proof-of-concept, the proposed model was validated by retrospectively predicting the expected efficacy at empirical DLPFC sites based on a large depression cohort and the outcome of two clinical cohorts (MDD and schizophrenia with AVH)
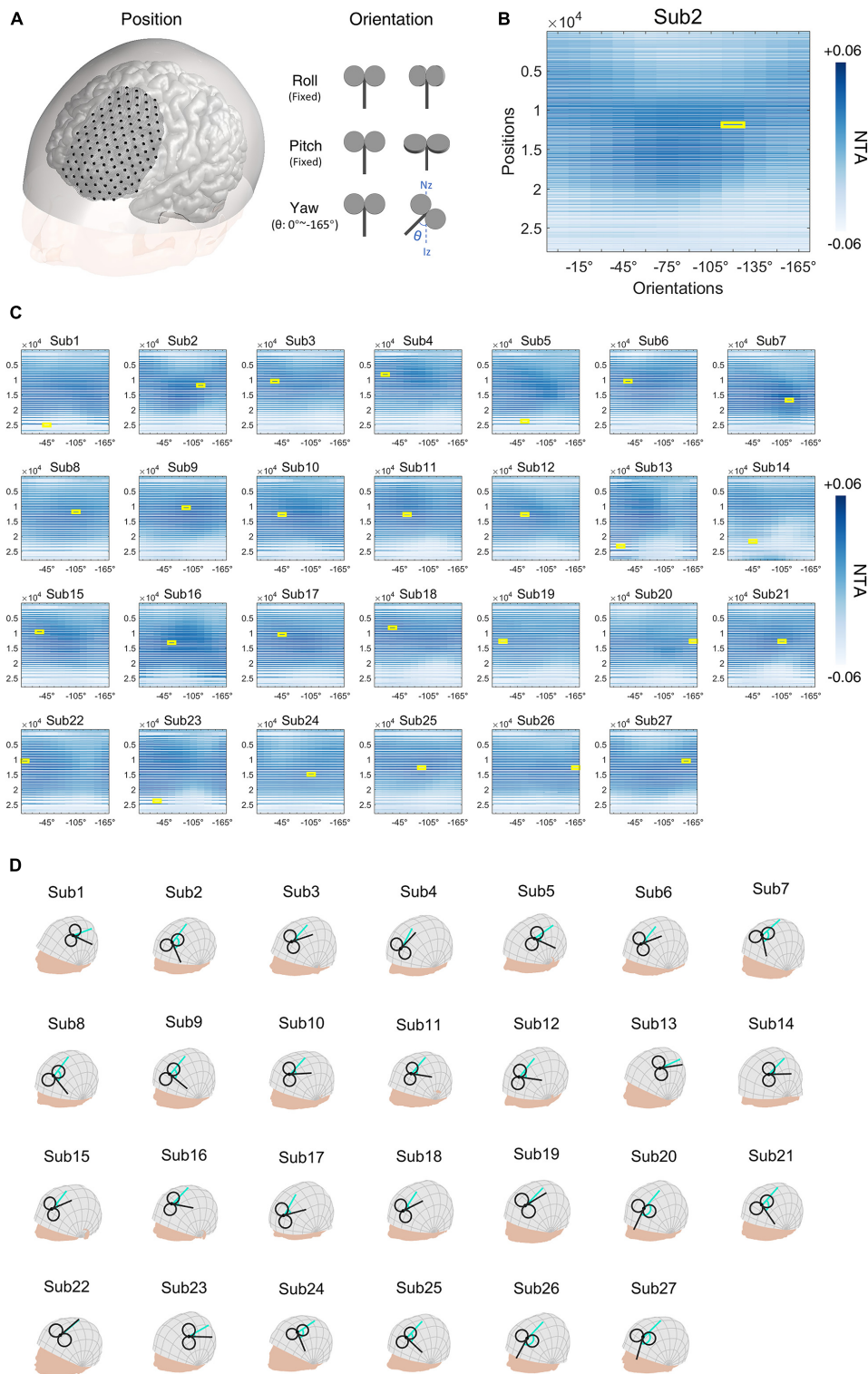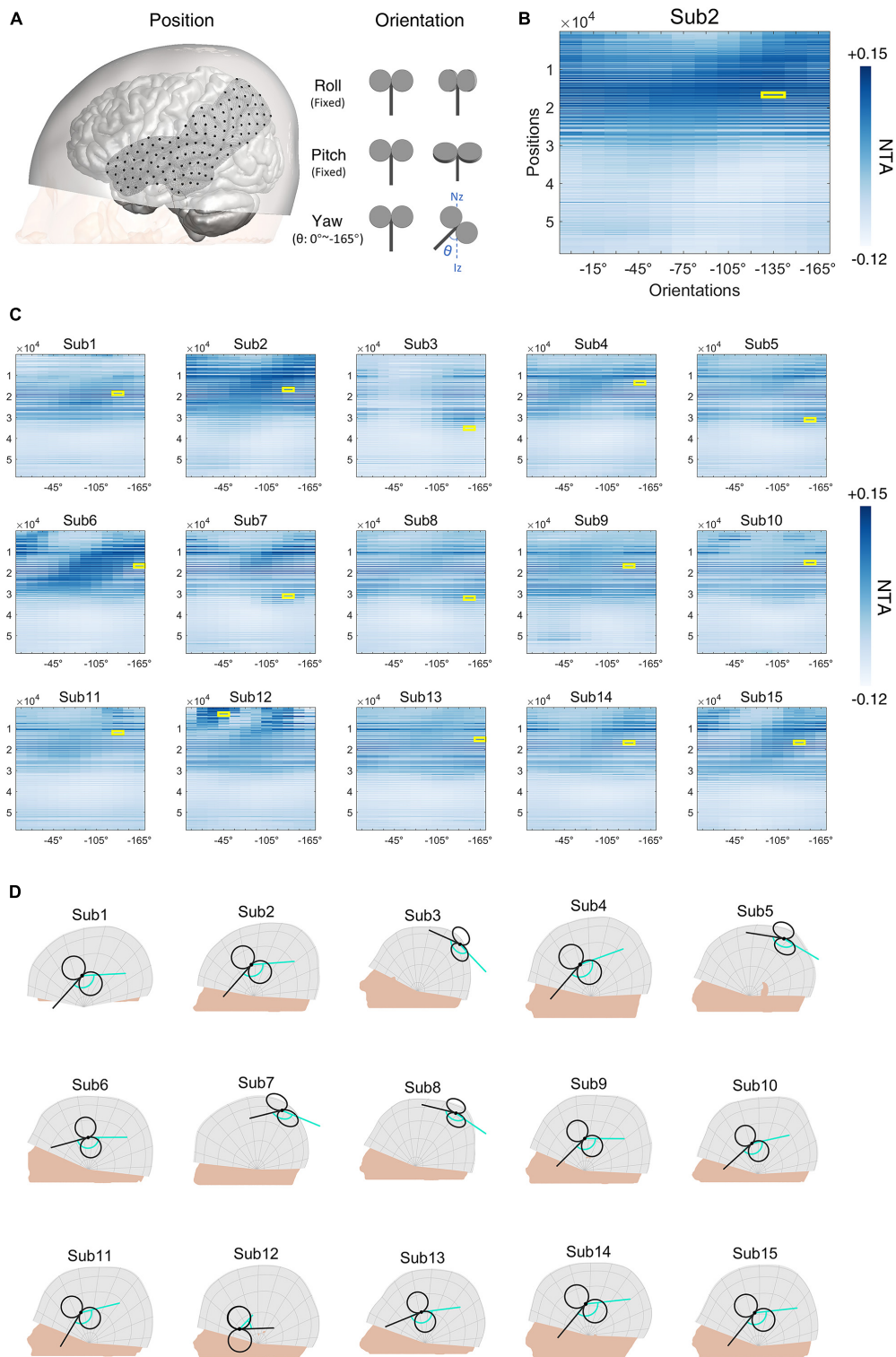
FIGURE 5

Major depressive disorder (MDD) simulation experiment. **(A)** Illustration of positions and orientations of a representative individual. Large black dots represent 125 positions in the search space. For each position, 12 coil orientations, in the normal plane at the position (0°∼−165°, 15-degree intervals), were tested. Network targeting accuracy (NTA) was calculated for each pair of position and orientation. **(B)** NTA value distribution in the search grid. Each position in the 2-D grid represents a combination of position and orientation. **(C)** Maximum NTA was found in all patients (yellow border). Search space was interpolated from 125 × 12 to 27,977 × 12 for visualization purposes. **(D)** The optimal transcranial magnetic stimulation (TMS) coil placements are shown in individual scalp spaces. The cyan arrow represents 0° at each position.

FIGURE 6

Schizophrenia with auditory verbal hallucinations (AVH) simulation experiment. **(A)** Illustration of positions and orientations of a representative individual. Large black dots represent the 122 positions in the search space. For each position, 12 coil orientations (0°∼−165°, 15-degree intervals) were tested. Network targeting accuracy (NTA) was calculated for each pair of position and orientation. **(B)** NTA value distribution in the search grid. Each position in the 2-D grid represents a combination of position and orientation. **(C)** Maximum NTA found in all patients (yellow border). Search space was interpolated from 122 × 12 to 58,470 × 12 for visualization purposes. **(D)** The optimal transcranial magnetic stimulation (TMS) coil placements are shown in individual scalp spaces. The cyan arrow represents 0° at each position.

TABLE 1 Symptom specificity of predictions from the network targeting accuracy (NTA) model.

Symptom scale	r	p
SAPS		
SAPS total	0.572*	0.013
AH1 (Auditory hallucinations)	0.590**	0.010
AH2 (Voices commenting)	0.585*	0.011
AH3 (Voices conversing)	0.834***	5.6×10^{-5}
Auditory hallucination total[†] (AH1+AH2+AH3)	0.633**	0.006
Hallucinations total	0.543*	0.018
Delusions total	−0.113	0.655
Bizarre behavior total	−0.073	0.602
Positive formal thought disorder total	0.064	0.411
SANS		
SANS total	0.021	0.470
Affective flattening	0.111	0.347
Alogia	0.124	0.329
Avolition apathy	0.313	0.128
Anhedonia associality	0.233	0.201
Attention	−0.054	0.576

[†]Sum of the SAPS hallucination subscale of schizophrenia with AVH items (sauditory hallucinations; voices commenting; voices conversing). *$p < 0.05$, **$p < 0.01$, ***$p < 0.001$.

that received TMS treatments. The proposed model significantly predicted treatment efficacy from the position and orientation of TMS parameters. Furthermore, in the cohort of schizophrenia with AVH, the prediction was both specific to the symptom corresponding to the targeted pathological network. Finally, we further applied the model to individual optimization of TMS parameters within the search space of traditional MDD and schizophrenia with AVH treatment on the scalp. The results of optimization showed the variance of optimal individual parameters and the interaction of position and orientation.

Consistent with related previous studies, our results demonstrated that considering both the local ROI and the related functional circuit affected by rTMS is a potential way to inform an accurate modulation for psychiatric disorders, in comparison to the traditional ROI-based approach. In a series of seminal studies in MDD, research has shown that the stimulation ROI of DLPFC with stronger anti-correlation with SGC tends to show better clinical improvement (Fox et al., 2012; Weigand et al., 2018; Cash et al., 2021a). While the mechanism is still unknown (Mayberg, 1997; Speer et al., 2000; Li et al., 2004; Padberg and George, 2009; Kito et al., 2011; Fox et al., 2012, 2014; Philip et al., 2018), the fact that SGC and DLPFC are two critical regions belonging to the frontal-limbic network, the putative pathological network of MDD identified by various neuroimaging studies, suggests that the information about the whole pathological network is necessary to inform effective TMS treatment. Comparing with other

targeting models, our model may have potential advantages in several aspects. First, most of the connectivity-based TMS targeting approaches focused on a single circuit based on prior knowledge, e.g., SCG-DLPFC for MDD. Our approach extended this notion by taking the collective effects on the whole pathological network into consideration. Compared with the SGC-DLPFC model (Fox et al., 2012), our model showed an improved prediction of treatment efficacy though to a limited extent (Supplementary Figure 8), indicating that other parts of the pathological network may add unique utility in guiding TMS coil setting. Second, in our model, the modulatory target was identified from the result of a large-sample meta-analysis. Compared to the hypothesis-driven method based on a specific ROI such as SGC for MDD (Fox et al., 2012; Weigand et al., 2018; Cash et al., 2019), the data-driven network targeting model is particular valuable for generalizing the prediction of treatment outcomes from MDD to other psychiatric disorders such as schizophrenia with AVH. Last but not the least, most of the targeting models do not take orientation of TMS coil into consideration (Fox et al., 2012; Weigand et al., 2018; Siddiqi et al., 2020; Cash et al., 2021b). However, it has been showm that the interaction between coil setting and individual's cortical anatomy impacts the E-field distribution at the stimulation target and bears individual differences of the modulatory effects imposed by TMS (Thielscher et al., 2011). Therefore, incorporating the E-field distribution should provide a more accurate estimation of the modulatory effect of TMS. In our simulation, the optimal combination of coil position and orientation varied among different patients, suggesting that by tuning the two simulation parameters together for individual patients may add efficacy for the TMS treatment.

For TMS-based treatment of schizophrenia with AVH, traditional targeting strategies are mainly based on a single-ROI target within the left temporoparietal cortex, either defined by anatomical landmarks such as TP3 (Hoffman et al., 2003) or left Wernicke (Hoffman et al., 2013), or functional foci showing abnormal activation (Sommer et al., 2007). Though techniques like neuronavigation have increased the accuracy in locating these ROIs, improvement in treatment efficacy is relatively limited (Slotema et al., 2011). Regarding this point, our retrospective analysis showed that minimizing the spatial distance to the targeted ROI was not related to treatment efficacy (Supplementary Figure 9). Instead, minimizing the functional distance to the pathological network of schizophrenia with AVH was shown to be a potential goal for optimization.

The interaction of position and orientation suggests the necessity of individual optimization. In the simple case, the MEP is highly dependent on coil position and orientation and an individual's intracranial anatomy (Windhoff et al., 2013; Laakso et al., 2014; Reijonen et al., 2020). In a more complicated case, the combination of coil position and orientation affects the targeting of functional networks (Opitz et al., 2016). In line with these studies, the proposed network targeting model also showed a significant interaction between coil location

and orientation on NTA. This suggests the necessity of including the coil orientation in both the parameter space and the individualized optimization process based on individual structural images.

In estimating the stimulation network of TMS, our results support the utility of group-level functional connectomes, as suggested in previous studies of similar functional connectome-based approaches (Fox et al., 2012, 2014; Weigand et al., 2018; Cash et al., 2019). It is worth noting that other evidence also suggests that the treatment efficacy of rTMS may be further improved by customizing stimulation sites based on individual differences in functional connectivity (Fox et al., 2013; Cash et al., 2019, 2021b). However, compared with individual functional connectivity, the advantage of using the normative connectome data is the generally higher signal-to-noise ratio. Data acquired on the normative population can be optimized by using improved technologies of acquisition, enlarging the sample size (Van Essen et al., 2012), and increasing the density of sampling in individuals (Laumann et al., 2015), which are usually difficult to conduct on patient populations (Horn and Fox, 2020). The trade-off between meaningful individual differences and the quality of functional connectivity data remains to be addressed in future work.

The proposed model derives the pathological network from the contrast of patient vs. healthy control. An implication is that reducing the biological deviation of the patient cohort from the healthy is a feasible direction for optimizing the parameters of TMS when treating mental disorders. Within such a model, further improvement can be made in several directions. This study used the altered baseline metabolic pattern of patients relative to healthy controls as the neural target for TMS-based treatment. As promising alternatives, symptom-specific pathological networks, compensatory networks, and side-effect networks for psychiatric diseases are worth considering in future studies. Psychiatric disorders are often diagnosed by heterogeneous symptoms, of which the biological markers are elusive (Abi-Dargham and Horga, 2016). Current efforts searching for neural markers of psychiatric disorders have identified distinct networks underlying the severity or the response to the treatment of psychiatric symptoms (Drysdale et al., 2017; Siddiqi et al., 2020). Therefore, nodes of these networks would be potential targets for the development of symptom-specific treatments. An interesting line of research focuses on identifying networks associated with treatment-induced side effects (Horn and Fox, 2020), and the results might be integrated into the proposed model as a "to-avoid" network in planning treatment. Apart from searching nodes of the pathological network, Balderston used a data-driven approach to link rsFC and symptoms of depression (Balderston et al., 2021), demonstrating the feasibility of edge-based targeting in TMS treatment. Such an edge-based pathological network will be considered in our model in the future.

There are several limitations to the current work. First, the sample size for the validation experiment was small. Therefore, the correlation analysis based on such a small sample might be unstable and result in a biased estimation of the true effect size. Second, the retrospective validation might be confounded by factors insufficiently controlled, e.g., variance in TMS protocols, heterogeneity of patients, or the way of selecting retrospective studies. Therefore, prospective validation would be necessary for follow-up research. Particularly, full-cycle studies are recommended, in which stimulation parameters are determined based on individual's MRI images and pathological network of the targeted disease or symptom before the TMS treatment is administrated. Third, though the proposed NTA model showed its ability to generalize to schizophrenia with AVH, a disease other than MDD, from which the core idea of the model arose, whether it can generalize to other psychiatric diseases need to be further investigated. Fourth, the current NTA model focused on TMS coil position and orientation, which are a subset of the TMS parameters. Other dimensions of the full parameter space such as the number of pulses, stimulation intensity, and temporal patterns of the pulses (Lefaucheur et al., 2014) need to be considered in future studies.

5 Conclusion

This study proposed a novel network targeting model for guiding individualized TMS treatment of psychiatric disorders. For a proof-of-concept, retrospective validation on MDD showed that the proposed model was capable of predicting clinical outcomes from TMS placement settings. The model showed comparable predictiveness for schizophrenia with AVH, demonstrating its generalizability. Finally, the proposed model showed potential for guiding individualized TMS placement. Though prospective validation is needed, this network targeting model may offer an opportunity for improving the current TMS-based treatment of psychiatric disorders.

Data availability statement

The cohorts, including the structure and resting-state functional MRI, used to construct the voxel-wise connectome are from the Southwest University Longitudinal Imaging Multimodal (SLIM) database (http://fcon_1000.projects.nitrc.org/indi/retro/southwestuni_qiu_index.html) and are openly available. The list of analyzed participants can be obtained upon request from CZ. The results of coordinate-based meta-analysis have been reported in studies published previously. The T1 images of the cohorts of MDD and schizophrenia with AVH are not publicly available due to the confidentiality policy of INSERM U A10 but are available upon reasonable request by contacting M-LP-M. The code used in the current study for developing the model is available upon reasonable request by contacting CZ. We share the code for making Figure 5. Please find the script on Github (https://github.com/Michaelcao92/NetworkTargetingVisualization). Further inquiries can be directed to the corresponding author.

Author contributions

ZC: conceptualization, formal analysis, methodology, investigation, visualization, data curation, software, and writing – original draft. XX: conceptualization, formal analysis, investigation, methodology, software, and writing – original draft. YZ: formal analysis and methodology. YJ, ZL, and ZD: writing – review and editing. CX: software. M-LP-M: resources and writing – review and editing. EA: resources. YY and CZ: funding acquisition, conceptualization, supervision, and writing – review and editing. All authors contributed to the article and approved the submitted version.

Funding

Acknowledgments

Conflict of interest

The authors declare that the research was conducted in the absence of any commercial or financial relationships that could be construed as a potential conflict of interest.

Publisher's note

Supplementary material

The Supplementary Material for this article can be found online at: https://www.frontiersin.org/articles/10.3389/fnins.2022.1079078/full#supplementary-material

References

Abi-Dargham, A., and Horga, G. (2016). The search for imaging biomarkers in psychiatric disorders. *Nat. Med.* 22, 1248–1255. doi: 10.1038/nm.4190

Anna Manelis, P. D., David, A. A., Baranger, P. D., Skye Satz, B. S., Rachel Ragozzino, M. A., Satish Iyengar, P. D., et al. (2021). Data from cortical myelin measured by the T1w/T2w ratio in individuals with depressive disorders and healthy controls. *OpenNeuro.* doi: 10.18112/openneuro.ds003653.v1.0.0

Balderston, N. L., Beer, J. C., Seok, D., Makhoul, W., Deng, Z., De, et al. (2021). Proof of concept study to develop a novel connectivity-based electric-field modelling approach for individualized targeting of transcranial magnetic stimulation treatment. *Neuropsychopharmacology* 47, 588–598. doi: 10.1038/s41386-021-01110-6

Barker, A. T., Jalinous, R., and Freeston, I. L. (1985). Non-invasive magnetic stimulation of human motor cortex. *Lancet* 325, 1106–1107. doi: 10.1016/S0140-6736(85)92413-4

Beam, W., Borckardt, J. J., Reeves, S. T., and George, M. S. (2009). An efficient and accurate new method for locating the F3 position for prefrontal TMS applications. *Brain Stimul.* 2, 50–54. doi: 10.1016/j.brs.2008.09.006

Bestmann, S., Ruff, C. C., Blankenburg, F., Weiskopf, N., Driver, J., and Rothwell, J. C. (2008). Mapping causal interregional influences with concurrent TMS–fMRI. *Exp. Brain Res.* 191, 383–402. doi: 10.1007/s00221-008-1601-8

Braun, U., Schaefer, A., Betzel, R. F., Tost, H., Meyer-Lindenberg, A., and Bassett, D. S. (2018). From maps to multi-dimensional network mechanisms of mental disorders. *Neuron* 97, 14–31. doi: 10.1016/j.neuron.2017.11.007

Cao, Z., Xiao, X., Zhao, Y., Jiang, Y., Xie, C., Paillère-Martinot, M.-L., et al. (2022). Targeting the pathological network?: Feasibility of network-based optimization of transcranial magnetic stimulation coil placement for treatment of psychiatric disorders short running title?: Pathological network targeting for TMS targeting the pathologic. *bioRxiv* [Preprint] doi: 10.1101/2022.10.23.513193

Cardenas, V. A., Bhat, J. V., Horwege, A. M., Ehrlich, T. J., Lavacot, J., Mathalon, D. H., et al. (2022). Anatomical and fMRI-network comparison of multiple DLPFC targeting strategies for repetitive transcranial magnetic stimulation treatment of depression. *Brain Stimul.* 15, 63–72. doi: 10.1016/j.brs.2021.11.008

Cash, R. F. H., Cocchi, L., Lv, J., Fitzgerald, P. B., and Zalesky, A. (2021a). Functional magnetic resonance imaging-guided personalization of transcranial magnetic stimulation treatment for depression. *JAMA Psychiatry* 78, 337–339. doi: 10.1001/jamapsychiatry.2020.3794

Cash, R. F. H., Cocchi, L., Lv, J., Wu, Y., Fitzgerald, P. B., and Zalesky, A. (2021b). Personalized connectivity-guided DLPFC-TMS for depression: Advancing computational feasibility, precision and reproducibility. *Hum. Brain Mapp.* 42, 4155–4172. doi: 10.1002/hbm.25330

Cash, R. F. H., Weigand, A., Zalesky, A., Siddiqi, S. H., Downar, J., Fitzgerald, P. B., et al. (2020). Using brain imaging to improve spatial targeting of transcranial magnetic stimulation for depression. *Biol. Psychiatry* 2, 1–8. doi: 10.1016/j.biopsych.2020.05.033

Cash, R. F. H., Zalesky, A., Thomson, R. H., Tian, Y., Cocchi, L., and Fitzgerald, P. B. (2019). Subgenual functional connectivity predicts antidepressant treatment response to transcranial magnetic stimulation: Independent validation and evaluation of personalization. *Biol. Psychiatry* 86, e5–e7. doi: 10.1016/j.biopsych.2018.12.002

Cho, S. S., and Strafella, A. P. (2009). rTMS of the left dorsolateral prefrontal cortex modulates dopamine release in the ipsilateral anterior cingulate cortex and orbitofrontal cortex. *PLoS One* 4:e6725. doi: 10.1371/journal.pone.0006725

Dayan, E., Censor, N., Buch, E. R., Sandrini, M., and Cohen, L. G. (2013). Noninvasive brain stimulation: From physiology to network dynamics and back. *Nat. Neurosci.* 16, 838–844. doi: 10.1038/nn.3422

De Deng, Z., Lisanby, S. H., and Peterchev, A. V. (2013). Electric field depth-focality tradeoff in transcranial magnetic stimulation: Simulation comparison of 50 coil designs. *Brain Stimul.* 6, 1–13. doi: 10.1016/j.brs.2012.02.005

Drysdale, A. T., Grosenick, L., Downar, J., Dunlop, K., Mansouri, F., Meng, Y., et al. (2017). Resting-state connectivity biomarkers define neurophysiological subtypes of depression. *Nat. Med.* 23, 28–38. doi: 10.1038/nm.4246

Eldaief, M. C., Halko, M. A., Buckner, R. L., and Pascual-Leone, A. (2011). Transcranial magnetic stimulation modulates the brain's intrinsic activity in a frequency-dependent manner. *Proc. Natl. Acad. Sci. U.S.A.* 108, 21229–21234. doi: 10.1073/pnas.1113103109

Fitzgerald, P. B. (2021). Targeting repetitive transcranial magnetic stimulation in depression: Do we really know what we are stimulating and how best to do it? *Brain Stimul.* 14, 730–736. doi: 10.1016/j.brs.2021.04.018

Fitzgerald, P. B., Hoy, K., McQueen, S., Maller, J. J., Herring, S., Segrave, R., et al. (2009). A randomized trial of rTMS targeted with MRI based neuro-navigation in treatment-resistant depression. *Neuropsychopharmacology* 34, 1255–1262. doi: 10.1038/npp.2008.233

Fitzgerald, P., Brown, T., Marston, N., Daskalakis, Z., Castella, A., De, et al. (2003). Transcranial magnetic stimulation in the treatment of depression during pregnancy. *Arch. Gen. Psychiatry* 60, 1002–1008. doi: 10.1001/archpsyc.60.9.1002

Fonov, V., Evans, A. C., Botteron, K., Almli, C. R., McKinstry, R. C., and Collins, D. L. (2011). Unbiased average age-appropriate atlases for pediatric studies. *Neuroimage* 54, 313–327. doi: 10.1016/j.neuroimage.2010.07.033

Fornito, A., and Bullmore, E. T. (2015). Connectomics: A new paradigm for understanding brain disease. *Eur. Neuropsychopharmacol.* 25, 733–748. doi: 10.1016/j.euroneuro.2014.02.011

Fox, M. D., and Raichle, M. E. (2007). Spontaneous fluctuations in brain activity observed with functional magnetic resonance imaging. *Nat. Rev. Neurosci.* 8, 700–711. doi: 10.1038/nrn2201

Fox, M. D., Buckner, R. L., Liu, H., Mallar Chakravarty, M., Lozano, A. M., and Pascual-Leone, A. (2014). Resting-state networks link invasive and noninvasive brain stimulation across diverse psychiatric and neurological diseases. *Proc. Natl. Acad. Sci. U.S.A.* 111, E4367–E4375. doi: 10.1073/pnas.1405003111

Fox, M. D., Buckner, R. L., White, M. P., Greicius, M. D., and Pascual-Leone, A. (2012). Efficacy of transcranial magnetic stimulation targets for depression is related to intrinsic functional connectivity with the subgenual cingulate. *Biol. Psychiatry* 72, 595–603. doi: 10.1016/j.biopsych.2012.04.028

Fox, M. D., Liu, H., and Pascual-Leone, A. (2013). Identification of reproducible individualized targets for treatment of depression with TMS based on intrinsic connectivity. *Neuroimage* 66, 151–160. doi: 10.1016/j.neuroimage.2012.10.082

Fox, P. T., Lancaster, J. L., Laird, A. R., and Eickhoff, S. B. (2014). Meta-analysis in human neuroimaging: Computational modeling of large-scale databases. *Annu. Rev. Neurosci.* 37, 409–434. doi: 10.1146/annurev-neuro-062012-170320

George, M. S., Ketter, T. A., and Post, R. M. (1994). Prefrontal cortex dysfunction in clinical depression. *Depression* 2, 59–72. doi: 10.1002/depr.3050020202

Gomez-Tames, J., Hamasaka, A., Laakso, I., Hirata, A., and Ugawa, Y. (2018). Atlas of optimal coil orientation and position for TMS: A computational study. *Brain Stimul.* 11, 839–848. doi: 10.1016/j.brs.2018.04.011

Gray, J. P., Müller, V. I., Eickhoff, S. B., and Fox, P. T. (2020). Multimodal abnormalities of brain structure and function in major depressive disorder: A meta-analysis of neuroimaging studies. *Am. J. Psychiatry* 177, 422–434. doi: 10.1176/appi.ajp.2019.19050560

Herbsman, T., Avery, D., Ramsey, D., Holtzheimer, P., Wadjik, C., Hardaway, F., et al. (2009). More lateral and anterior prefrontal coil location is associated with better repetitive transcranial magnetic stimulation antidepressant response. *Biol. Psychiatry* 66, 509–515. doi: 10.1016/j.biopsych.2009.04.034

Herwig, U., Satrapi, P., and Schönfeldt-Lecuona, C. (2003). Using the international 10-20 EEG system for positioning of transcranial magnetic stimulation. *Brain Topogr.* 16, 95–99. doi: 10.1023/B:BRAT.0000006333.93597.9d

Herwig, U., Schönfeldt-Lecuona, C., Wunderlich, A. P., Von Tiesenhausen, C., Thielscher, A., Walter, H., et al. (2001). The navigation of transcranial magnetic stimulation. *Psychiatry Res. Neuroimaging* 108, 123–131. doi: 10.1016/S0925-4927(01)00121-4

Hoffman, R. E., Hawkins, K. A., Gueorguieva, R., Boutros, N. N., Rachid, F., Carroll, K., et al. (2003). Transcranial magnetic stimulation of left temporoparietal cortex and medication-resistant auditory hallucinations. *Arch. Gen. Psychiatry* 60, 49–56. doi: 10.1001/archpsyc.60.1.49

Hoffman, R. E., Wu, K., Pittman, B., Cahill, J. D., Hawkins, K. A., Fernandez, T., et al. (2013). Transcranial magnetic stimulation of wernicke's and right homologous sites to curtail voices: A randomized trial. *Biol. Psychiatry* 73, 1008–1014. doi: 10.1016/j.biopsych.2013.01.016

Horn, A., and Fox, M. D. (2020). Opportunities of connectomic neuromodulation. *Neuroimage* 221:117180. doi: 10.1016/j.neuroimage.2020.117180

Howard, J. D., Reynolds, R., Smith, D. E., Voss, J. L., Schoenbaum, G., and Kahnt, T. (2020). Targeted stimulation of human orbitofrontal networks disrupts outcome-guided behavior. *Curr. Biol.* 30, 490–498.e4. doi: 10.1016/j.cub.2019.12.007

Jiang, Y., Du, B., Chen, Y., Wei, L., Cao, Z., Zong, Z., et al. (2022). A scalp-measurement based parameter space: Towards locating TMS coils in a clinically-friendly way. *Brain Stimul.* 15, 924–926. doi: 10.1016/j.brs.2022.06.001

Kito, S., Hasegawa, T., and Koga, Y. (2011). Neuroanatomical correlates of therapeutic efficacy of low-frequency right prefrontal transcranial magnetic stimulation in treatment-resistant depression. *Psychiatry Clin. Neurosci.* 65, 175–182. doi: 10.1111/j.1440-1819.2010.02183.x

Klirova, M., Horacek, J., Novak, T., Cermak, J., Spaniel, F., Skrdlantova, L., et al. (2013). Individualized rTMS neuronavigated according to regional brain metabolism (18FGD PET) has better treatment effects on auditory hallucinations than standard positioning of rTMS: A double-blind, sham-controlled study. *Eur. Arch. Psychiatry Clin. Neurosci.* 263, 475–484. doi: 10.1007/s00406-012-0368-x

Kühn, S., and Gallinat, J. (2012). Quantitative meta-analysis on state and trait aspects of auditory verbal hallucinations in schizophrenia. *Schizophr. Bull.* 38, 779–786. doi: 10.1093/schbul/sbq152

Laakso, I., Hirata, A., and Ugawa, Y. (2014). Effects of coil orientation on the electric field induced by TMS over the hand motor area. *Phys. Med. Biol.* 59, 203–218. doi: 10.1088/0031-9155/59/1/203

Laumann, T. O., Gordon, E. M., Adeyemo, B., Snyder, A. Z., Joo, S. J., Chen, M. Y., et al. (2015). Functional system and areal organization of a highly sampled individual human brain. *Neuron* 87, 657–670. doi: 10.1016/j.neuron.2015.06.037

Lefaucheur, J. P., André-Obadia, N., Antal, A., Ayache, S. S., Baeken, C., Benninger, D. H., et al. (2014). Evidence-based guidelines on the therapeutic use of repetitive transcranial magnetic stimulation (rTMS). *Clin. Neurophysiol.* 125, 2150–2206. doi: 10.1016/j.clinph.2014.05.021

Li, X., Nahas, Z., Kozel, F. A., Anderson, B., Bohning, D. E., and George, M. S. (2004). Acute left prefrontal transcranial magnetic stimulation in depressed patients is associated with immediately increased activity in prefrontal cortical as well as subcortical regions. *Biol. Psychiatry* 55, 882–890. doi: 10.1016/j.biopsych.2004.01.017

Liu, W., Wei, D., Chen, Q., Yang, W., Meng, J., Wu, G., et al. (2017). Longitudinal test-retest neuroimaging data from healthy young adults in southwest China. *Sci. Data* 4, 1–9. doi: 10.1038/sdata.2017.17

Liuzzi, L., Chang, K., Keren, H., Zheng, C., Saha, D., Nielson, D., et al. (2021). Data from: Mood induction in MDD and healthy adolescents. *OpenNeuro*. doi: 10.18112/openneuro.ds003568.v1.0.2

Mayberg, H. S. (1997). Limbic-cortical dysregulation: A proposed model of depression. *J. Neuropsychiatr.* 9, 471–481. doi: 10.1176/appi.pn.2013.5a10

Okamoto, M., Dan, H., Sakamoto, K., Takeo, K., Shimizu, K., Kohno, S., et al. (2004). Three-dimensional probabilistic anatomical cranio-cerebral correlation via the international 10-20 system oriented for transcranial functional brain mapping. *Neuroimage* 21, 99–111. doi: 10.1016/j.neuroimage.2003.08.026

Opitz, A., Fox, M. D., Craddock, R. C., Colcombe, S., and Milham, M. P. (2016). An integrated framework for targeting functional networks via transcranial magnetic stimulation. *Neuroimage* 127, 86–96. doi: 10.1016/j.neuroimage.2015.11.040

Padberg, F., and George, M. S. (2009). Repetitive transcranial magnetic stimulation of the prefrontal cortex in depression. *Exp. Neurol.* 219, 2–13. doi: 10.1016/j.expneurol.2009.04.020

Paillère Martinot, M. L., Galinowski, A., Ringuenet, D., Gallarda, T., Lefaucheur, J. P., Bellivier, F., et al. (2010). Influence of prefrontal target region on the efficacy of repetitive transcranial magnetic stimulation in patients with medication-resistant depression: A [18F]-fluorodeoxyglucose PET and MRI study. *Int. J. Neuropsychopharmacol.* 13, 45–59. doi: 10.1017/S146114570900008X

Paillère-Martinot, M. L., Galinowski, A., Plaze, M., Andoh, J., Bartrés-Faz, D., Bellivier, F., et al. (2017). Active and placebo transcranial magnetic stimulation effects on external and internal auditory hallucinations of schizophrenia. *Acta Psychiatr. Scand.* 135, 228–238. doi: 10.1111/acps.12680

Pascual-Leone, A., Rubio, B., Pallardó, F., and Catalá, M. D. (1996). Rapid-rate transcranial magnetic stimulation of left dorsolateral prefrontal cortex in drug-resistant depression. *Lancet* 348, 233–237. doi: 10.1016/S0140-6736(96)01219-6

Pascual-Leone, A., Tormos, J. M., Keenan, J., Tarazona, F., Cañete, C., and Catalá, M. D. (1998). Study and modulation of human cortical excitability with transcranial magnetic stimulation. *J. Clin. Neurophysiol.* 15, 333–343. doi: 10.1097/00004691-199807000-00005

Paus, T., Castro-Alamancos, M. A., and Petrides, M. (2001). Cortico-cortical connectivity of the human mid-dorsolateral frontal cortex and its modulation by repetitive transcranial magnetic stimulation. *Eur. J. Neurosci.* 14, 1405–1411. doi: 10.1046/j.0953-816X.2001.01757.x

Philip, N. S., Barredo, J., van 't Wout-Frank, M., Tyrka, A. R., Price, L. H., and Carpenter, L. L. (2018). Network mechanisms of clinical response to transcranial magnetic stimulation in posttraumatic stress disorder and major depressive disorder. *Biol. Psychiatry* 83, 263–272. doi: 10.1016/j.biopsych.2017.07.021

Rajkowska, G., and Goldman-Rakic, P. S. (1995). Cytoarchitectonic definition of prefrontal areas in normal human cortex: I. Remapping of areas 9 and 46 and relationship to the Talairach coordinate system. *Cereb. Cortex* 5, 307–322. doi: 10.1093/cercor/5.4.323

Reijonen, J., Säisänen, L., Könönen, M., Mohammadi, A., and Julkunen, P. (2020). The effect of coil placement and orientation on the assessment of focal excitability in motor mapping with navigated transcranial magnetic stimulation. *J. Neurosci. Methods* 331:108521. doi: 10.1016/j.jneumeth.2019.108521

Reithler, J., Peters, J. C., and Sack, A. T. (2011). Multimodal transcranial magnetic stimulation: Using concurrent neuroimaging to reveal the neural network dynamics of noninvasive brain stimulation. *Prog. Neurobiol.* 94, 149–165. doi: 10.1016/j.pneurobio.2011.04.004

Richter, L., Neumann, G., Oung, S., Schweikard, A., and Trillenberg, P. (2013). Optimal coil orientation for transcranial magnetic stimulation. *PLoS One* 8:e60358. doi: 10.1371/journal.pone.0060358

Rossini, P. M., Rossini, L., and Ferreri, F. (2010). Transcranial magnetic stimulation: A review. *IEEE Eng. Med. Biol. Mag.* 29, 84–95. doi: 10.1109/MEMB.2009.935474

Rusjan, P. M., Barr, M. S., Farzan, F., Arenovich, T., Maller, J. J., Fitzgerald, P. B., et al. (2010). Optimal transcranial magnetic stimulation coil placement for targeting the dorsolateral prefrontal cortex using novel magnetic resonance image-guided neuronavigation. *Hum. Brain Mapp.* 31, 1643–1652. doi: 10.1002/hbm.20964

Sale, M. V., Mattingley, J. B., Zalesky, A., and Cocchi, L. (2015). Imaging human brain networks to improve the clinical efficacy of non-invasive brain stimulation. *Neurosci. Biobehav. Rev.* 57, 187–198. doi: 10.1016/j.neubiorev.2015.09.010

Saturnino, G. B., Puonti, O., Nielsen, J. D., Antonenko, D., Madsen, K. H., and Thielscher, A. (2019). "SimNIBS 2.1: A comprehensive pipeline for individualized electric field modelling for transcranial brain stimulation," in *Brain and human body modeling*, eds S. Makarov, M. Horner, and G. Noetscher (Cham: Springer), 3–25. doi: 10.1007/978-3-030-21293-3_1

Siddiqi, S. H., Taylor, S. F., Cooke, D., Pascual-Leone, A., George, M. S., and Fox, M. D. (2020). Distinct symptom-specific treatment targets for circuit-based neuromodulation. *Am. J. Psychiatry* 177, 435–446. doi: 10.1176/appi.ajp.2019.19090915

Silbersweig, D. A., Stern, E., Frith, C., Cahill, C., Holmes, A., Grootoonk, S., et al. (1995). A functional neuroanatomy of hallucinations in schizophrenia. *Nature* 378, 176–179. doi:10.1038/378176a0

Slotema, C. W., Blom, J. D., Weijer, A. D., De, Diederen, K. M., Goekoop, R., et al. (2011). Can low-frequency repetitive transcranial magnetic stimulation really relieve medication-resistant auditory verbal hallucinations?? Negative results from a large randomized controlled trial. *Biol. Psychiatry* 69, 450–456. doi: 10.1016/j.biopsych.2010.09.051

Sommer, I. E. C., Slotema, C. W., de Weijer, A. D., Blom, J. D., Daalman, K., Neggers, S. F., et al. (2007). Can fMRI-guidance improve the efficacy of rTMS treatment for auditory verbal hallucinations? *Schizophr. Res.* 93, 406–408. doi: 10.1016/j.schres.2007.03.020

Speer, A. M., Kimbrell, T. A., Wassermann, E. M., Repella, J. D., Willis, M. W., Herscovitch, P., et al. (2000). Opposite effects of high and low frequency rTMS on regional brain activity in depressed patients. *Biol. Psychiatry* 48, 1133–1141. doi: 10.1016/S0006-3223(00)01065-9

Thielscher, A., Antunes, A., and Saturnino, G. B. (2015). "Field modeling for transcranial magnetic stimulation: A useful tool to understand the physiological effects of TMS?," in *Proceedings of the 2015 37th annual international conference of the IEEE engineering in medicine and biology society (EMBC)* (Milan: IEEE), 222–225. doi: 10.1109/EMBC.2015.7318340

Thielscher, A., Opitz, A., and Windhoff, M. (2011). Impact of the gyral geometry on the electric field induced by transcranial magnetic stimulation. *Neuroimage* 54, 234–243. doi: 10.1016/j.neuroimage.2010.07.061

Thomson, R. H., Cleve, T. J., Bailey, N. W., Rogasch, N. C., Maller, J. J., Daskalakis, Z. J., et al. (2013). Blood oxygenation changes modulated by coil orientation during prefrontal transcranial magnetic stimulation. *Brain Stimul.* 6, 576–581. doi: 10.1016/j.brs.2012.12.001

Tik, M., Hoffmann, A., Sladky, R., Tomova, L., Hummer, A., Navarro, et al. (2017). Towards understanding rTMS mechanism of action: Stimulation of the DLPFC causes network-specific increase in functional connectivity. *Neuroimage* 162, 289–296. doi: 10.1016/j.neuroimage.2017.09.022

Van Essen, D. C., Ugurbil, K., Auerbach, E., Barch, D., Behrens, T. E. J., Bucholz, R., et al. (2012). The human connectome project: A data acquisition perspective. *Neuroimage* 62, 2222–2231. doi: 10.1016/j.neuroimage.2012.02.018

Wang, J. X., Rogers, L. M., Gross, E. Z., Ryals, A. J., Dokucu, M. E., Brandstatt, K. L., et al. (2014). Memory enhancement: Targeted enhancement of cortical-hippocampal brain networks and associative memory. *Science* 345, 1054–1057. doi: 10.1126/science.1252900

Weigand, A., Horn, A., Caballero, R., Cooke, D., Stern, A. P., Taylor, S. F., et al. (2018). Prospective Validation that subgenual connectivity predicts antidepressant efficacy of transcranial magnetic stimulation sites. *Biol. Psychiatry* 84, 28–37. doi: 10.1016/j.biopsych.2017.10.028

Windhoff, M., Opitz, A., and Thielscher, A. (2013). Electric field calculations in brain stimulation based on finite elements: An optimized processing pipeline for the generation and usage of accurate individual head models. *Hum. Brain Mapp.* 34, 923–935. doi: 10.1002/hbm.21479

Xiao, X., Yu, X., Zhang, Z., Zhao, Y., Jiang, Y., Li, Z., et al. (2018). Transcranial brain atlas. *Sci. Adv.* 4:eaar6904. doi: 10.1126/sciadv.aar6904